Cureus
Part of SPRINGER NATURE

Open Access Original Article

Comparative Evaluation of Pterion Morphology and Morphometry in Dry Human Skulls and Craniolateral Computed Tomography: An Osteological and Radiological Study

Review began 10/03/2026
Review ended 10/13/2026
Published 10/23/2026

© **Copyright** 2026
Choudhary et al. This is an open access article distributed under the terms of the Creative Commons Attribution License CC-BY 4.0., which permits unrestricted use, distribution, and reproduction in any medium, provided the original author and source are credited.

DOI: 10.7759/cureus.118459

Rinke Choudhary [1], Surekha Waghanna [1], Prasad Hegde [2], Avinash Munshi [2], Renu Chahun [3], Kumar Satish Ravi [1], Sangita Chauhan [1]

1. Anatomy, National Institute of Medical Sciences and Research, Jaipur, IND 2. Radiology, National Institute of Medical Sciences and Research, Jaipur, IND 3. Anatomy, University College of Medical Sciences and Guru Teg Bahadur (GTB) Hospital, Delhi, IND

Corresponding author: Surekha Waghanna, drsurekha.patil11@yahoo.com

Abstract

Introduction: The pterion is a craniometric landmark overlying the anterior division of the middle meningeal artery and the lateral (Sylvian) fissure. Its variation is relevant to pterional neurosurgery and to the interpretation of cranial sutures on imaging. Osteological and computed tomography (CT) data obtained within a single study are limited.

Objective: The objective of the study is to compare pterion morphology, and its distances from the zygomaticotemporal suture (Cp-ZT) and the frontozygomatic suture (Cp-FZ), between independent samples of adult dry human skulls and adult three-dimensional CT examinations, and between sides.

Materials and methods: In this comparative cross-sectional study (April 2024 to October 2025), 118 adult dry skulls and 118 adult cranial CT examinations, obtained from different individuals, were assessed bilaterally (236 sides per dataset) after an a priori sample-size estimate. Each side was classified as sphenoparietal, epipteric, stellate, frontotemporal, or atypical. Cp-ZT and Cp-FZ were measured with a digital Vernier calliper on skulls and with the electronic calliper of the imaging software on CT reconstructions. Distributions were compared with the Pearson chi-squared or Fisher-Freeman-Halton exact test and distances with the independent-samples t-test (significance, $p < 0.05$).

Results: The sphenoparietal type predominated in both datasets (dry skulls 61.0%; CT 68.6% of sides). The right-sided distribution did not differ between datasets ($\chi^2 = 6.00$, $p = 0.199$), whereas the left-sided distribution did ($\chi^2 = 16.29$, exact $p = 0.002$), chiefly because epipteric bones were recorded more often in skulls than in the CT dataset (22.9% vs 8.5%). Values below are dry skull vs CT. Cp-ZT was shorter in the CT dataset on both sides (right 33.83 vs 25.69 mm; left 31.88 vs 27.10 mm; both $p < 0.001$). Cp-FZ was longer in the CT dataset on the right (26.66 vs 29.27 mm, $p < 0.001$) and marginally shorter on the left (25.75 vs 24.80 mm, $p = 0.031$).

Conclusions: The sphenoparietal type predominated in both datasets and on both sides, and the right-sided distributions were similar. The left-sided distribution and the absolute distances differed between datasets. Because the skulls and CT examinations came from different individuals and the two measurement methods are not geometrically equivalent, these differences cannot be attributed to imaging modality alone and may also reflect population, age, and sex differences. The lower frequency of epipteric bones in the CT dataset is consistent with limited CT depiction of fine sutures, but this hypothesis needs testing on paired CT and osteological examinations of the same crania. Reference values from the two sources should not be combined without qualification.

Categories: Radiology, Orthopedics, Anatomy
Keywords: anatomical variation, computed tomography, dry human skull, middle meningeal artery, morphometry, pterion, pterional approach

Introduction

The pterion is an H-shaped or K-shaped sutural junction on the lateral aspect of the skull at which the frontal bone, the parietal bone, the squamous part of the temporal bone, and the greater wing of the sphenoid bone meet. It corresponds developmentally to the site of the anterolateral (sphenoidal) fontanelle, and its adult configuration is established during postnatal growth as the adjacent bones approximate and articulate [1,2]. Because these bones ossify and grow at different rates, the final pattern of articulation at the pterion is variable, and this variability has both developmental and population-specific determinants [3,4].

The clinical significance of the pterion relates to its underlying neurovascular and cortical relations. The internal surface of the pterional region is grooved by the anterior division of the middle meningeal artery, and the pterion overlies the lateral (Sylvian) fissure and the adjacent inferior frontal and anterior temporal cortex [1,2]. In most adults, the pterion lies within a circle of 1 cm diameter centred approximately 2.6 cm posterior and 1.3 cm superior to the posterolateral margin of the frontozygomatic suture, and this area overlies the anterior branch of the middle meningeal artery in about two-thirds of cases [2]. The adjacent squamous temporal bone is thin, and the region is therefore a recognised site of extradural haemorrhage following temporal trauma. The pterion is also the principal surface landmark for the pterional (frontotemporosphenoidal) craniotomy used to access the anterior and middle cranial fossae, the circle of Willis, and parasellar lesions. Accurate knowledge of its position and configuration is therefore considered important for burr-hole placement, craniotomy planning, and avoidance of injury to the middle meningeal artery [2,5].

Following the classification proposed by Murphy, the pterion is conventionally grouped into four principal sutural types: sphenoparietal (direct sphenoparietal articulation), frontotemporal (direct frontotemporal articulation), stellate (convergence of four bones at a single point), and epipteric (one or more intervening sutural (Wormian) bones) [3]. The epipteric pattern is of particular radiological relevance because accessory sutural bones and their surrounding sutures may be misinterpreted as fracture lines on cranial imaging and may lead the surgeon to select an incorrect, excessively anterior landmark [5,6]. The reported prevalence of the four types varies considerably between populations, and a heritable component of the sutural pattern has been demonstrated in a pedigreed primate population [4].

Pterion morphology and morphometry have traditionally been studied on dry skulls, which permit direct inspection of sutures and precise calliper measurement. Computed tomography (CT), particularly three-dimensional surface reconstruction, allows the same landmark to be evaluated non-invasively in living individuals within intact craniofacial anatomy, and CT has been used to characterise the pterion and its sutural variants for the lateral neurosurgical approach [6,7]. However, spatial resolution, slice thickness, and partial-volume averaging may limit the recognition of fine sutural detail, so osteological and radiological findings cannot be assumed to be equivalent [6].

Few studies have reported pterion morphology and morphometry from both dry skulls and CT within the same investigation. Such data would show how far findings from the two sources resemble one another and would provide reference values for imaging and surgery. The present study therefore compared pterion morphology and morphometry between adult dry human skulls and three-dimensional CT images. The two samples were drawn from different individuals, so the comparison is between two independent datasets and not between two modalities applied to the same crania.

Materials And Methods

Aim, objectives, and hypothesis

Aim

The aim of the study is to compare pterion morphology and morphometry between independent samples of adult dry human skulls and adult three-dimensional craniolateral CT examinations, and between sides.

Primary Objective

The primary objective is to compare, on each side, the distribution of pterion types (sphenoparietal, epipteric, stellate, frontotemporal, and atypical) between the dry-skull and CT datasets.

Secondary Objective

The secondary objective is to compare, on each side, the distance from the centre of the pterion (Cp) to the zygomaticotemporal suture (Cp-ZT) and to the frontozygomatic suture (Cp-FZ) between the two datasets.

Hypothesis

The null hypothesis was that the distribution of pterion types and the distances Cp-ZT and Cp-FZ do not differ between the dry-skull and CT datasets. Because the datasets are independent, any difference is interpreted as a difference between datasets, not as a measure of imaging performance or diagnostic agreement.

Study design, setting, and period

This comparative cross-sectional study combined osteological and radiological assessment of the pterion and was conducted over 18 months, from April 2024 to October 2025, after approval by the Institutional Ethics Committee on March 19, 2024. A total of 118 adult dry human skulls of unknown age and sex were

examined: 24 from the teaching collection of the Department of Anatomy, National Institute of Medical Sciences and Research (NIMS University Rajasthan), Jaipur, and 94 from the Department of Anatomy, University College of Medical Sciences (UCMS) and Guru Teg Bahadur Hospital, Delhi. Osteological data at UCMS were collected between April 15, 2024, and April 1, 2025, under the supervision of the Head of the Department of Anatomy, UCMS, and osteological data at NIMS were collected within the study period. In parallel, 118 adult cranial CT examinations performed for unrelated clinical indications were retrieved retrospectively during the study period from the picture archiving and communication system (PACS) of the Department of Radiology, NIMS Tertiary Care Hospital, Jaipur. Each skull and each CT examination was assessed bilaterally, giving 236 sides per dataset. Because the skulls and CT examinations were obtained from different individuals and, in part, from different institutions, the study compares two independent groups and not paired observations on the same crania.

The study was approved by the Institutional Ethics Committee of NIMS University Rajasthan, Jaipur (Ref. No. NIMSUR/IEC/2024/929; Proposal No. IEC/P-583/2024). The dry skulls were unidentified specimens from institutional teaching collections, and the CT examinations were anonymised before analysis, so that no identifiable patient information was accessed. The study was conducted in accordance with the principles of the Declaration of Helsinki.

Sample size

The sample size was estimated a priori using the formula for estimating the difference between two independent means with a specified absolute precision [8]: $n = Z\alpha/2^2 (\sigma1^2 + \sigma2^2)/d^2$, where $Z\alpha/2 = 1.96$ corresponds to a 95% confidence level; $\sigma1 = 2.2$ mm and $\sigma2 = 2.5$ mm are the standard deviations (SD) of the pterion-frontozygomatic distance reported for the right and left sides, respectively, in a previous CT study by Singh et al. [9]; and $d = 0.6$ mm is the required precision (half-width of the 95% confidence interval (CI) of the mean difference). Substitution gave $n = 1.96^2 \times (2.2^2 + 2.5^2)/0.6^2 = 118.34$, and a sample of 118 per group was adopted. Accordingly, 118 dry skulls and 118 cranial CT examinations were included. The estimate was based on the precision of a continuous distance, and the comparisons of pterion type were not separately powered. The CT examinations were selected by convenience sampling: eligible examinations available in the PACS during the study period were included until the calculated sample size of 118 was reached.

Inclusion and exclusion criteria

Dry skulls were included when both pterional regions were intact and the constituent sutures were clearly preserved. Skulls from which the calvaria had been removed (46 of the UCMS skulls) were included only when both pterional regions and both zygomatic arches were intact. Skulls were excluded when they were of juvenile age or showed incomplete suture closure, when the temporal or zygomatic region was fractured or deformed, or when the sutures were obliterated or affected by a congenital anomaly. CT examinations were included when both pterional regions were clearly visualised with adequate image quality, and were excluded when they were of paediatric patients, demonstrated a cranial fracture or a pathological lesion involving the pterional region, or were of inadequate quality.

Instruments, equipment, and software

Osteological measurements were made with a calibrated digital stainless-steel Vernier calliper (resolution 0.1 mm). Cranial CT examinations were acquired on a SOMATOM Scope scanner (Siemens Healthineers, Erlangen, Germany) operating on syngo CT VC30 software, with a tube voltage of 110 kVp, a tube current of 140 mA, and a gantry rotation time of 1 s. Three-dimensional surface-rendered reconstructions were reviewed, and radiological measurements were performed, in Horos version 3.3.6 (open-source DICOM viewer; Horos Project, sponsored by Nimble Co LLC d/b/a Purview, Annapolis, MD, USA). Statistical analysis was performed with IBM SPSS Statistics for Windows, version 21.0 (IBM Corp., Armonk, NY, USA).

Morphological assessment

In dry skulls, the pterion was inspected macroscopically on each side under adequate illumination. On CT, bilateral craniolateral three-dimensional surface-rendered images were reconstructed and reviewed. Using the criteria of Murphy [3], each side was classified as sphenoparietal (direct sphenoparietal contact), frontotemporal (direct frontotemporal contact), stellate (four bones meeting at a point), or epipteric (one or more intervening sutural bones) (Figure *1*). Configurations that did not conform to any of these four categories, such as ambiguous, composite, or partially fused junctions, were recorded separately as an atypical pattern. All specimens and images were classified independently by two observers, and disagreements were resolved by consensus.

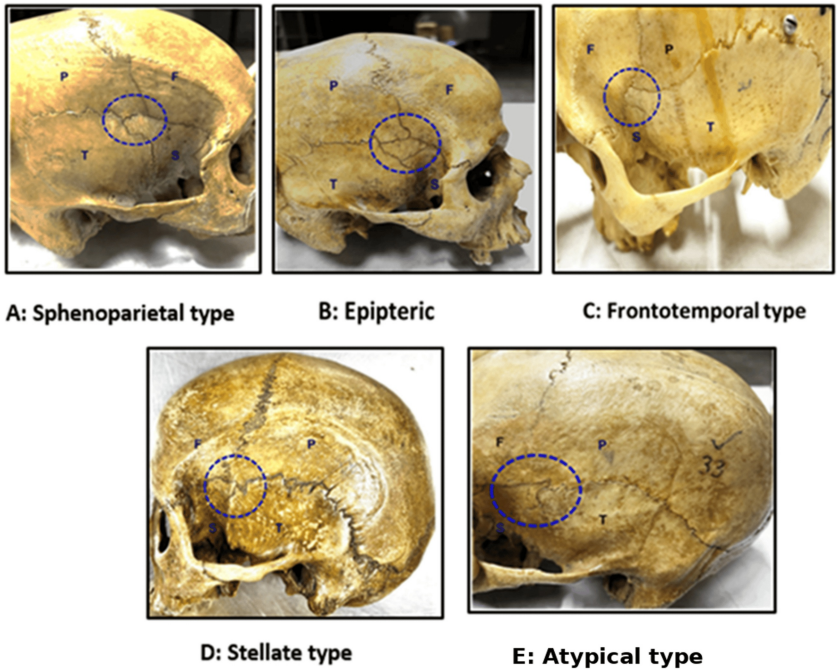


FIGURE 1: Morphological types of the pterion in dry human skulls

Dashed circles indicate the pterion. (A) Sphenoparietal, (B) epipteric, (C) frontotemporal, (D) stellate, and (E) atypical (non-classical) type.

F: frontal bone; P: parietal bone; T: temporal bone; S: greater wing of the sphenoid bone

Morphometric assessment

The Cp was defined as the point of confluence of the articulating bones. Two linear distances were recorded on each side (Figure *2*): the distance from Cp to the zygomaticotemporal suture (Cp-ZT) and the distance from Cp to the frontozygomatic suture (Cp-FZ). In dry skulls, distances were measured with the digital Vernier calliper, which records the direct straight-line distance between two landmarks. On CT, the same landmarks were identified on the three-dimensional reconstruction and measured with the electronic calliper tool of the imaging software, which records a distance within the displayed view. The two methods are therefore not geometrically identical. Each measurement was taken twice, and the mean of the two readings was used for analysis. All measurements were expressed in millimetres.

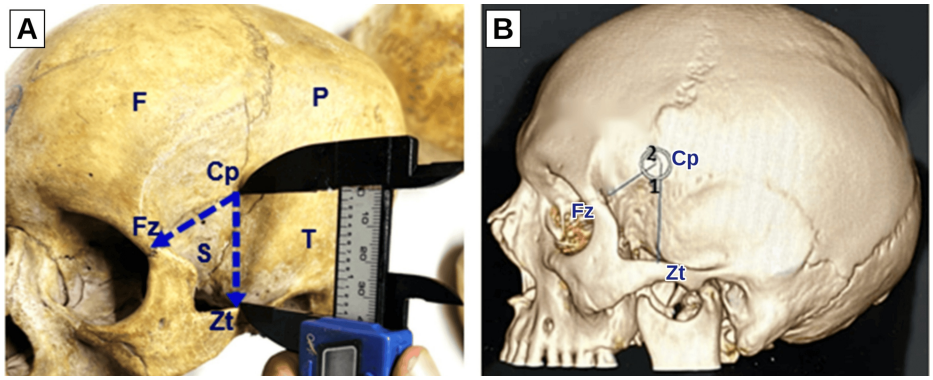


FIGURE 2: Measurement of pterion morphometry

(A) Dry skull, lateral view, showing measurement with a digital Vernier calliper; dashed arrows indicate the distances from the centre of the pterion (Cp) to the frontozygomatic suture (Fz; Cp-FZ) and to the zygomaticotemporal suture (Zt; Cp-ZT). (B) Three-dimensional surface-rendered CT reconstruction (craniolateral view) showing the same landmarks; the pterion is circled, line 1 indicates Cp-ZT and line 2 indicates Cp-FZ, both measured with the electronic calliper tool of the imaging software. Landmark labels were added for legibility.

F: frontal bone; P: parietal bone; T: temporal bone; S: greater wing of the sphenoid bone; CT: computed tomography

Statistical analysis

Categorical variables were summarised as frequencies and percentages and continuous variables as mean ± SD. The two sides of a skull are not independent observations. To avoid treating them as independent, the morphological distribution and the distances were compared between the dry-skull and CT datasets separately for each side, and pooled percentages across sides are presented descriptively only. Because the skulls and CT examinations came from different individuals, the two datasets are independent groups, and a within-subject analysis across datasets was not possible. Models that account for within-skull correlation, such as generalised estimating equations or mixed-effects models, are an alternative approach; they were not used in the primary analysis.

For each side, the morphological distribution was compared between datasets using the Pearson chi-squared test; when more than 20% of cells had an expected count below 5, or a cell count was zero, the Fisher-Freeman-Halton exact test was used. The strength of association was expressed as Cramér's V. Continuous morphometric variables were compared between datasets with the independent-samples t-test, which is robust to moderate departures from normality at this sample size; the magnitude of each difference was expressed as the mean difference with its 95% CI and as Cohen's d. A two-tailed p-value < 0.05 was considered statistically significant.

Results

The 118 dry skulls and 118 CT examinations provided 236 sides per modality for analysis. The composition of the study material is summarised in Table *1*.

Material	Source	Specimens (n)	Sides assessed (n)
Dry human skulls	NIMS, Jaipur	24	48
	UCMS, Delhi (48 complete skulls; 46 skulls without calvaria)	94	188
Cranial CT examinations	NIMS Tertiary Care Hospital, Jaipur	118	236
Total	All sources	236	472

TABLE 1: Composition of the study material

CT: computed tomography; NIMS: National Institute of Medical Sciences & Research; UCMS: University College of Medical Sciences

Morphological findings

Representative examples of each morphological type in dry skulls are shown in Figure 1. The sphenoparietal type was the most frequent configuration in both datasets and on both sides. Because the two sides of a skull are not independent observations, formal comparisons between datasets were performed separately for each side.

Right Side

On the right side, the sphenoparietal type was observed in 75/118 skulls (63.6%) and 80/118 CT examinations (67.8%). The remaining types differed only modestly between datasets, the largest difference being in the epipteric type (18.6% vs 10.2%), and the right-sided distribution did not differ significantly between dry skulls and CT ($\chi^2 = 6.00$, $p = 0.199$; Cramér's V = 0.16) (Table 2, Figures 3, 4).

Pterion type	Dry skull, n (%)	CT, n (%)
Sphenoparietal	75 (63.6)	80 (67.8)
Epipteric	22 (18.6)	12 (10.2)
Stellate	7 (5.9)	13 (11.0)
Frontotemporal	2 (1.7)	4 (3.4)
Atypical	12 (10.2)	9 (7.6)
Total	118 (100)	118 (100)

TABLE 2: Right-sided pterion morphology in dry skulls versus CT (n = 118 each)

Pearson chi-squared test: χ^2 (df = 4) = 6.00, p = 0.199 (Fisher-Freeman-Halton exact p = 0.198); Cramér's V = 0.16. The test statistic applies to the whole distribution and is therefore shown once for the table. p > 0.05, not significant.

CT: computed tomography; df: degrees of freedom

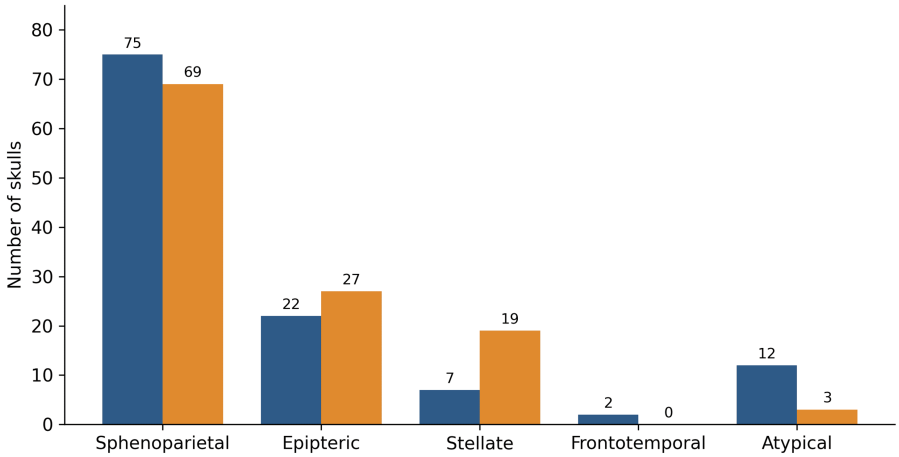


FIGURE 3: Side-wise distribution of pterion morphological types in dry human skulls (n = 118)

Blue bars, right side; orange bars, left side. Values above the bars are numbers of skulls.

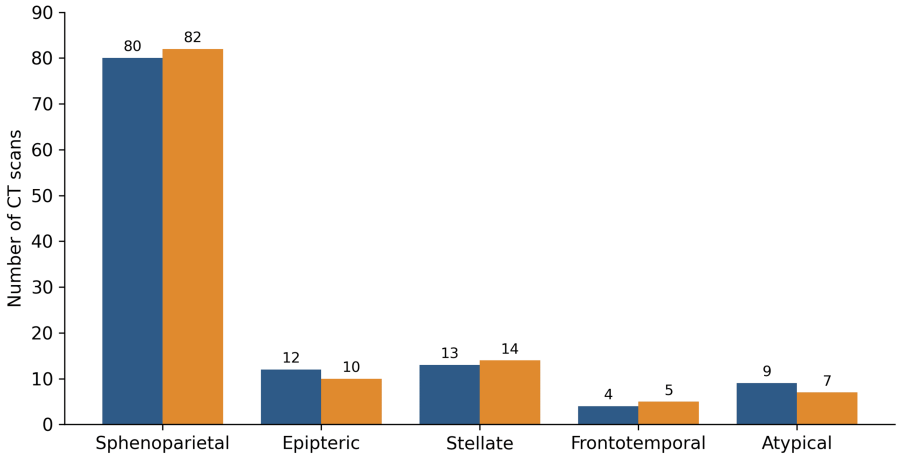


FIGURE 4: Side-wise distribution of pterion morphological types on CT scans (n = 118)

Blue bars, right side; orange bars, left side. Values above the bars are numbers of CT examinations.

CT: computed tomography

Left Side

On the left side, the sphenoparietal type was again predominant (69/118 skulls, 58.5%; 82/118 CT examinations, 69.5%). The left-sided distribution, however, differed significantly between datasets (χ^2 = 16.29, Fisher-Freeman-Halton exact p = 0.002; Cramér's V = 0.26). The difference was attributable chiefly to the epipteric type, which was recorded more frequently in skulls (27/118, 22.9%) than in the CT dataset (10/118, 8.5%); the frontotemporal type was absent in skulls but present on five CT examinations (4.2%), and the atypical type was slightly more frequent on CT (Table *3*, Figures *3*, *4*).

Pterion type	Dry skull, n (%)	CT, n (%)
Sphenoparietal	69 (58.5)	82 (69.5)
Epipteric	27 (22.9)	10 (8.5)
Stellate	19 (16.1)	14 (11.9)
Frontotemporal	0 (0.0)	5 (4.2)
Atypical	3 (2.5)	7 (5.9)
Total	118 (100)	118 (100)

TABLE 3: Left-sided pterion morphology in dry skulls versus CT (n = 118 each)

Fisher-Freeman-Halton exact test: χ^2 (df = 4) = 16.29, p = 0.002; Cramér's V = 0.26. The exact test was used because of a zero cell and small expected counts (Pearson chi-squared p = 0.003). The test statistics apply to the whole distribution and are therefore shown once for the table. p < 0.05, significant.

CT: computed tomography; df: degrees of freedom

Side-Wise Comparison

Within each dataset, the sphenoparietal type remained predominant on both sides. The distribution of the less common variants nevertheless differed between sides in dry skulls: the epipteric (22 vs 27) and stellate (7 vs 19) types were more frequent on the left, whereas the atypical type was more frequent on the right (12 vs 3). In the CT dataset, the two sides were closely similar (Figures *3*, *4*). These side-wise differences were not tested formally.

Overall Distribution

Pooled across the 236 sides per dataset, the sphenoparietal type accounted for 61.0% of dry-skull sides and 68.6% of CT sides, followed by the epipteric (20.8% vs 9.3%), stellate (11.0% vs 11.4%), atypical (6.4% vs 6.8%), and frontotemporal (0.8% vs 3.8%) patterns (Figure 5). Because the two sides of a skull are not independent, these pooled percentages are presented descriptively.

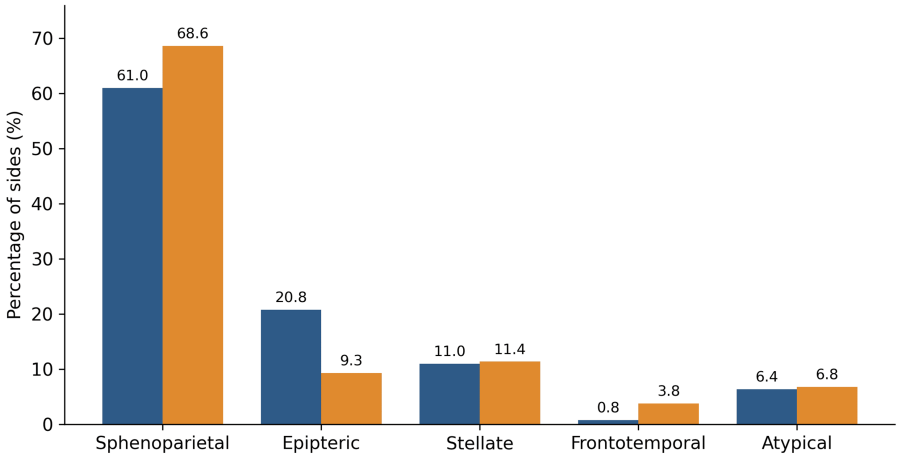


FIGURE 5: Overall pterion morphology in dry skulls versus CT (236 sides per modality)

Blue bars, dry skulls; orange bars, CT. Values above the bars are percentages of assessed sides and are presented descriptively. The sphenoparietal type predominates in both modalities; the epipteric type is less frequent on CT.

CT: computed tomography

Morphometric findings

Cp-ZT and Cp-FZ were measured as illustrated in Figure 2, and the differences between datasets are summarised in Table 4 and Figure 6. Cp-ZT was significantly greater in dry skulls than in the CT dataset on both sides (right 33.83 ± 3.92 mm vs 25.69 ± 3.69 mm, mean difference 8.14 mm, $p < 0.001$; left 31.88 ± 3.70 mm vs 27.10 ± 4.14 mm, mean difference 4.78 mm, $p < 0.001$), with large effect sizes. Cp-FZ differed in a side-dependent manner: it was shorter in skulls than in the CT dataset on the right (26.66 ± 4.76 mm vs 29.27 ± 3.50 mm, $p < 0.001$; medium effect) and marginally longer in skulls on the left (25.75 ± 3.14 mm vs 24.80 ± 3.59 mm; mean difference 0.95 mm, $p = 0.031$; small effect). The two datasets therefore yielded significantly different absolute positional measurements of the pterion, most markedly for Cp-ZT.

Parameter	Side	Dry skull (mean ± SD)	CT (mean ± SD)	Mean difference (95% CI)	t	p-value	Cohen's d
Cp-ZT	Right	33.83 ± 3.92	25.69 ± 3.69	8.14 (7.16 to 9.12)	16.42	<0.001	2.14
Cp-ZT	Left	31.88 ± 3.70	27.10 ± 4.14	4.78 (3.77 to 5.79)	9.35	<0.001	1.22
Cp-FZ	Right	26.66 ± 4.76	29.27 ± 3.50	−2.61 (−3.68 to −1.54)	−4.80	<0.001	−0.63
Cp-FZ	Left	25.75 ± 3.14	24.80 ± 3.59	0.95 (0.09 to 1.82)	2.16	0.031	0.28

TABLE 4: Pterion morphometry (mm) in dry skulls versus CT

Independent-samples t-test, n = 118 per group (df = 234). Mean difference = dry skull − CT. Cohen's d: approximately 0.2 small, 0.5 medium, and ≥ 0.8 large.

Cp-ZT: centre of pterion to zygomaticotemporal suture; Cp-FZ: centre of pterion to frontozygomatic suture; SD: standard deviation; CI: confidence interval; CT: computed tomography; df: degrees of freedom

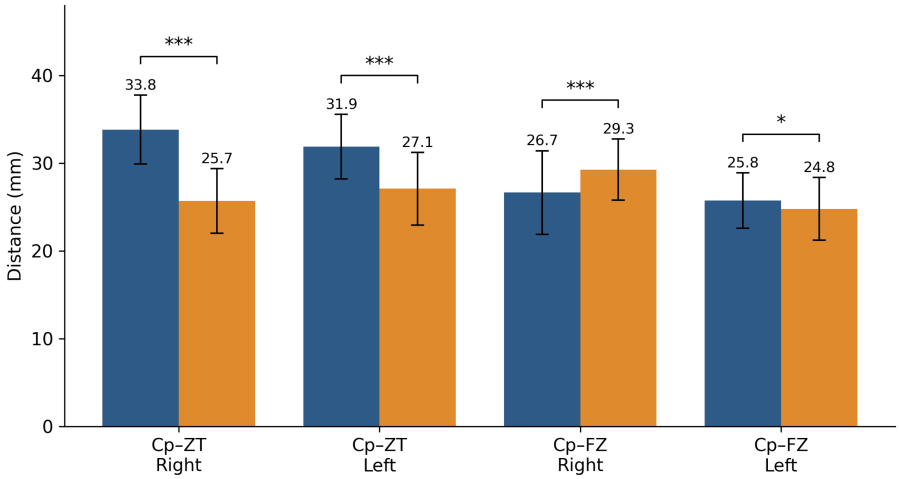


FIGURE 6: Pterion morphometry in dry skulls versus CT (mean ± SD)

Blue bars, dry skulls; orange bars, CT. Bars show means, error bars indicate SD, and values above the bars are means (mm).

*p < 0.05; ***p < 0.001 (independent-samples t-test).

Cp-ZT: centre of pterion to zygomaticotemporal suture; Cp-FZ: centre of pterion to frontozygomatic suture; SD: standard deviation; CT: computed tomography

Discussion

This study compared pterion morphology and morphometry between an osteological sample and a CT sample drawn from different individuals. Three principal findings emerged. First, the sphenoparietal type predominated in both datasets and on both sides. Second, the morphological distributions were similar on the right but differed significantly on the left, principally because epipteric bones were recorded more frequently in dry skulls than in the CT dataset. Third, the absolute positional measurements (Cp-ZT and Cp-FZ) differed significantly between datasets. Because the skulls and CT examinations came from different individuals and the age and sex of the skulls were unknown, these differences cannot be attributed to imaging modality alone. They may also reflect differences between the source populations, demographic composition, and the measurement methods.

The predominance of the sphenoparietal type is consistent with the majority of osteological and radiological series [10-14]. Reported sphenoparietal prevalence ranges from approximately 62% to more than 90%: 92.4% on CT in Pakistani men [7], 81.2% in Thai skulls [10], 70%-75% in dry Indian skulls [15], 86.1% in Nigerian skulls [12], 87.5% in Turkish male skulls [13], and 62.1% in a second Thai series [16]. A meta-analysis of 79 studies comprising 18,694 skull sides reported a pooled sphenoparietal prevalence of 78.5%, followed by the epipteric (8.4%), frontotemporal (5.7%), and stellate (4.3%) types [17]. The sphenoparietal prevalence in the present study (61.0% in skulls and 68.6% in the CT dataset) lies at the lower end of this range. The sphenoparietal type ranked first in both datasets, as in the pooled estimate, and the epipteric type ranked second in dry skulls; in the CT dataset, however, the stellate type (11.4%) slightly exceeded the epipteric type (9.3%). The osteological prevalence of the epipteric type (20.8%) exceeded the pooled estimate but was comparable with the values of 17.4% in Thai skulls [10] and 16% in the skull series of Ma et al. [2]. Stellate junctions (11.0%-11.4%) were more frequent, and frontotemporal junctions (0.8%-3.8%) less frequent, than the pooled estimates. Figure 7 compares the present sphenoparietal prevalence with published data.

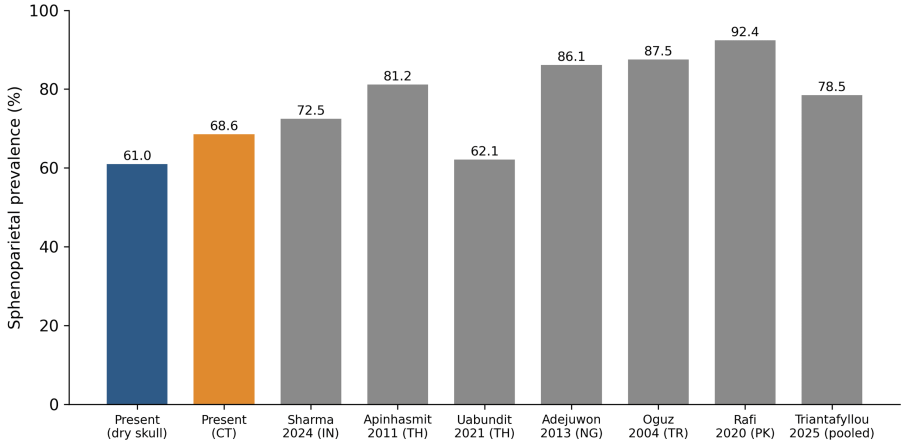


FIGURE 7: Sphenoparietal pterion prevalence in the present study compared with published series

Grey bars represent previously reported values [7,10,12,13,15-17]; blue and orange bars represent the present dry-skull and CT results, respectively.

IN: India; TH: Thailand; NG: Nigeria; TR: Turkey; PK: Pakistan; CT: computed tomography

The significant left-sided difference between the datasets is the most notable finding of this study. The epipteric pattern was recorded in 22.9% of left-sided skulls but in only 8.5% of left-sided CT examinations. One possible explanation is that, on three-dimensional surface-rendered CT, the fine sutures bounding epipteric (Wormian) bones may be obscured by limited spatial resolution, slice thickness, reconstruction smoothing, and partial-volume averaging, so that an epipteric junction is classified as sphenoparietal or atypical. This explanation is a hypothesis, and the present design cannot test it, because the skulls and CT examinations were obtained from different individuals and no paired comparison on the same crania was made. Other explanations include differences between the source populations, age- and sex-related variation (fusion of the pterion and its epipteric bones has been related to age [18]), and observer-dependent classification. Using multidetector CT angiography with three-dimensional reconstruction, Çalışkan et al. emphasised that sutural variants may be misinterpreted as fractures, and they recorded such variants least frequently at the left pterion [6], an observation in the same direction as the low left-sided CT frequency of epipteric bones in the present series. The direction of the difference in our data, with more epipteric bones in skulls and more frontotemporal and atypical junctions in the CT dataset, is compatible with the resolution hypothesis but does not establish it. Paired CT and osteological examination of the same crania is needed to determine whether CT under-detects epipteric bones.

The epipteric type is of potential clinical significance. In a series of 490 skull sides, Ersoy et al. found epipteric bones in 9% and showed that, when such a bone is present, the most anterior bony junction may be misidentified as the pterion, resulting in burr-hole placement as close as 16 mm to the lateral orbital rim and a risk of inadvertent orbital penetration [5]. Radiologically, the accessory sutures surrounding an epipteric bone may mimic a linear fracture in the setting of trauma [6]. If CT does depict epipteric bones less often than direct inspection, as our data suggest but cannot prove, such errors could be more likely when CT is the sole basis of assessment. The present study did not evaluate surgical accuracy, diagnostic performance, or clinical outcomes, so these implications are drawn from the literature and remain speculative.

An atypical, non-classical configuration was recorded in a minority of sides (7.6%-10.2% on the right and 2.5%-5.9% on the left). Murphy's classification recognises four types [3], but composite or intermediate junctions do not always conform to these categories. Matsumura et al. described several subtypes of sphenoparietal and frontotemporal contact and documented age-related fusion of the pterion and its epipteric bones, indicating that pterion morphology represents a developmental continuum rather than four discrete states [18]. A heritable contribution to this variation has been demonstrated in a pedigreed rhesus monkey population [4]. The atypical category in the present study should be interpreted in this context; as a residual category, it inevitably includes borderline classifications and is observer-dependent.

The morphometric findings require cautious interpretation. Cp-ZT was consistently shorter in the CT dataset than in skulls, whereas Cp-FZ differed in a side-dependent manner. A substantial part of this discrepancy may be methodological. A Vernier calliper records the direct straight-line distance between two landmarks in three dimensions and is independent of skull orientation, whereas an electronic calliper applied to a surface-rendered image displayed in a single craniolateral view records a two-dimensional

distance in the viewing plane; segments that are not parallel to that plane are foreshortened, and the result depends on the orientation of the reconstruction, which CT studies commonly standardise to the Frankfort horizontal plane [7]. Landmark identification may also differ, because suture ends are less distinct on rendered images than on bone. The two techniques may therefore not measure identical geometric distances, and the large Cp-ZT differences, particularly on the right, may reflect measurement method more than true differences between samples. The present design cannot separate these effects. Ma et al. likewise reported slightly greater distances between the pterion and the frontozygomatic suture on cone-beam CT than in dry skulls (29 vs 26 mm horizontally and 16 vs 11 mm vertically) [2]. CT-derived and osteologically derived positional reference values should not be combined without qualification. Published pterion-frontozygomatic distances in dry skulls, approximately 31 mm in Thai and Nigerian series [10,12] and 33-34 mm in Turkish men [13], exceed the present osteological Cp-FZ values (25.8-26.7 mm), which probably reflects population differences and the reference point chosen on the suture. Distances to the zygomatic arch, approximately 38-40 mm in dry skulls [10,12,13] and 34.5 mm on CT [7], are not directly comparable with Cp-ZT because a different inferior reference point was used.

The inclusion of both an osteological and a CT dataset in one investigation is the principal strength of this study. Osteological examination provides an unobstructed, high-resolution view of the sutures and of accessory bones and is therefore suited to prevalence estimates and anthropological studies. CT, in contrast, allows the same landmark to be studied in living patients within intact craniofacial anatomy, which is relevant to surgical planning and radiological practice [6,7,17,19]. The two sources address different questions. In the present samples, findings were similar for the dominant type and for the right-sided distribution but differed for minor variants and for absolute distances; whether this reflects the imaging technique, the source populations, or both cannot be determined from this design. Patient-specific CT is the practical means of localising the pterion before a pterional approach [5,17], and the present data suggest that distances measured on rendered CT may differ from osteological reference values.

Because age and sex were not available for the dry skulls, sexual dimorphism was not analysed, and the age and sex composition of the CT cohort could not be compared with that of the skulls. The type and position of the pterion are known to vary with sex and age [10,16]; complete pterional synostosis was observed only in male skulls in one series [16], and fusion of the pterion and its epipteric bones has been related to age [18]. Differences in age and sex between the two datasets could therefore account for part of the observed differences, in addition to or instead of any effect of the imaging technique. The conclusions of the present study are accordingly limited to differences between these two datasets. Within these limits, and if the lower frequency of epipteric bones in the CT dataset reflects limited depiction of fine sutures, radiologists should interpret complex pterional sutures with this possibility in mind, and CT-based pterion localisation should be regarded as a guide whose absolute distances may differ from osteological reference values.

Limitations

This study has several limitations. The most important is its independent-group design. The dry skulls and CT examinations were obtained from different individuals and, in part, from different institutions and regions (skulls from Jaipur and Delhi; CT from Jaipur). The study therefore compares two datasets, not two modalities applied to the same crania, and differences between the datasets may reflect differences between the source populations rather than the imaging technique. Without paired CT and osteological assessment of the same specimens, the study cannot establish the diagnostic performance of CT, the agreement between the two approaches, or whether CT under-detects epipteric bones.

Second, age and sex were not available for the dry skulls, and the demographic profile of the CT cohort was not compared with them, which precludes analysis of age- and sex-related variation and leaves it unclear how much of the between-dataset difference is attributable to demographic composition. Third, the two measurement techniques are not geometrically equivalent: a Vernier calliper records a three-dimensional straight-line distance, whereas the electronic calliper on a surface-rendered image records a distance in the displayed view, which depends on image orientation and landmark identification. Part of the differences in Cp-ZT and Cp-FZ may therefore be methodological.

Fourth, the CT examinations were selected by convenience sampling from a single centre, which may limit generalisability, and the sample size was calculated for the precision of a distance measurement, so the comparisons of pterion type were not separately powered. Fifth, although each specimen and image was classified independently by two observers with consensus resolution, assignment to the atypical category is inherently observer-dependent. Sixth, the depiction of fine sutural detail on three-dimensional CT depends on spatial resolution, slice thickness, and reconstruction parameters, and the retrospective design did not permit an acquisition protocol optimised for sutural anatomy. Seventh, the two sides of a skull are correlated; sides were analysed separately, and models that account for within-skull correlation were not used in the primary analysis, and the side-wise differences within each dataset were described but not tested.

Finally, the study did not evaluate surgical accuracy, diagnostic performance, operative outcomes, or clinical utility, and the relationship of the pterion to the underlying middle meningeal artery and to intracranial landmarks was not examined. The clinical implications discussed above are therefore inferential.

Conclusions

In these independent samples of adult dry skulls and craniolateral CT examinations, the sphenoparietal type was the predominant pterion configuration on both sides, and the right-sided distributions were similar. The left-sided distribution differed between the datasets, mainly because epipteric bones were recorded less often in the CT dataset, and the absolute measurements of pterion position (Cp-ZT and Cp-FZ) also differed. Because the skulls and CT examinations came from different individuals, the two measurement techniques are not geometrically equivalent, and age and sex of the skulls were unavailable; these differences cannot be attributed to imaging modality alone. A lower frequency of epipteric bones on CT is consistent with limited depiction of fine sutures, but this remains a hypothesis to be tested on paired CT and osteological examinations of the same crania. Until then, CT-derived and osteologically derived pterion data should be interpreted separately, reference values from the two sources should not be combined without qualification, and the implications for radiological interpretation of cranial sutures and for pterional neurosurgical planning remain inferential.

Additional Information

Author Contributions

All authors have reviewed the final version to be published and agreed to be accountable for all aspects of the work.

Concept and design: Sangita Chauhan, Surekha Waghanna, Prasad Hegde, Avinash Munshi, Renu Chahun, Kumar Satish Ravi, Rinke Choudhary

Acquisition, analysis, or interpretation of data: Sangita Chauhan, Surekha Waghanna, Rinke Choudhary

Drafting of the manuscript: Sangita Chauhan, Surekha Waghanna, Prasad Hegde, Avinash Munshi, Renu Chahun, Kumar Satish Ravi, Rinke Choudhary

Critical review of the manuscript for important intellectual content: Sangita Chauhan, Surekha Waghanna, Prasad Hegde, Avinash Munshi, Renu Chahun, Kumar Satish Ravi, Rinke Choudhary

Supervision: Surekha Waghanna

Disclosures

Human subjects: Informed consent for treatment and open access publication was obtained or waived by all participants in this study. National Institute of Medical Sciences and Research, NIMS University Rajasthan issued approval NIMSUR/IEC/2024/929. **Animal subjects:** All authors have confirmed that this study did not involve animal subjects or tissue. **Conflicts of interest:** In compliance with the ICMJE uniform disclosure form, all authors declare the following: **Payment/services info:** All authors have declared that no financial support was received from any organization for the submitted work. **Financial relationships:** All authors have declared that they have no financial relationships at present or within the previous three years with any organizations that might have an interest in the submitted work. **Other relationships:** All authors have declared that there are no other relationships or activities that could appear to have influenced the submitted work.

References

1. Standring S: Gray's Anatomy: The Anatomical Basis of Clinical Practice. Elsevier, Edinburgh; 2020.
2. Ma S, Baillie LJ, Stringer MD: Reappraising the surface anatomy of the pterion and its relationship to the middle meningeal artery. Clin Anat. 2012, 25:330-9. 10.1002/ca.21232
3. Murphy T: The pterion in the Australian aborigine. Am J Phys Anthropol. 1956, 14:225-44. 10.1002/ajpa.1330140218
4. Wang Q, Opperman LA, Havill LM, Carlson DS, Dechow PC: Inheritance of sutural pattern at the pterion in Rhesus monkey skulls. Anat Rec A Discov Mol Cell Evol Biol. 2006, 288:1042-9. 10.1002/ar.a.20373
5. Ersoy M, Evliyaoglu C, Bozkurt MC, Konuskan B, Tekdemir I, Keskil IS: Epipteric bones in the pterion may be a surgical pitfall. Minim Invasive Neurosurg. 2003, 46:363-5. 10.1055/s-2003-812434
6. Çalışkan S, Oğuz KK, Tunalı S, Aldur MM, Erçakmak B, Sargon MF: Morphology of cranial sutures and radiologic evaluation of the variations of intersutural bones. Folia Morphol (Warsz). 2018, 77:730-5. 10.5603/FM.a2018.0030
7. Rafi A, Sayeed S, Anwar MI: Cranial CT scan evaluation of morphological variations and location of pterion in Pakistani male population for lateral neurosurgical approach. Pak J Med Sci. 2020, 36:310-5. 10.12669/pjms.36.3.2003
8. Kirkwood BR, Sterne JA: Calculation of required sample size. Essential Medical Statistics. Blackwell Science, Oxford; 2003.
9. Singh AK, Modi V, Kumar M, Arfat M: Cranial CT scan evaluation of morphological variations of bony pattern & location of pterion in the Indore male population for a lateral neurosurgical approach. J Xi'an Shiyou Univ Nat Sci Ed. 2023, 19:187-97.
10. Apinhasmit W, Chompoopong S, Chaisuksunt V, Thiraphatthanavong P, Phasukdee N: Anatomical

consideration of pterion and its related references in Thai dry skulls for pterional surgical approach. J Med Assoc Thai. 2011, 94:205-14.
11. Mwachaka PM, Hassanali J, Odula P: Sutural morphology of the pterion and asterion among adult Kenyans . Braz J Morphol Sci. 2009, 26:4-7.
12. Adejuwon SA, Olopade FE, Bolaji M: Study of the location and morphology of the pterion in adult Nigerian skulls. ISRN Anat. 2013, 2013:403937. 10.5402/2013/403937
13. Oguz O, Sanli SG, Bozkir MG, Soames RW: The pterion in Turkish male skulls . Surg Radiol Anat. 2004, 26:220-4. 10.1007/s00276-003-0210-2
14. Saxena RC, Bilodi AK, Mane SS, Kumar A: Study of pterion in skulls of Awadh area--in and around Lucknow . Kathmandu Univ Med J (KUMJ). 2003, 1:32-3.
15. Sharma R, Vaibhav V, Meshram R, Khorwal G, Singh B, Bhardwaj Y: Morphometric evaluation of sutural patterns at the pterion and Asterion in dry Indian skulls: surgical relevance. Cureus. 2024, 16:e54466. 10.7759/cureus.54466
16. Uabundit N, Chaiyamoon A, Iamsaard S, Yurasakpong L, Nantasenamat C, Suwannakhan A, Phunchago N: Classification and morphometric features of pterion in Thai population with potential sex prediction . Medicina (Kaunas). 2021, 57:1282. 10.3390/medicina57111282
17. Triantafyllou G, Karangeli N, Duparc F, et al.: Unveiling pterion variability: a meta-analytic approach to enhance neurosurgical precision. Surg Radiol Anat. 2025, 47:66. 10.1007/s00276-025-03571-6
18. Matsumura G, Kida K, Ichikawa R, Kodama G: Pterion and epipteric bones in Japanese adults and fetuses, with special reference to their formation and variations (Article in Japanese). Kaibogaku Zasshi. 1991, 66:462-71.
19. Aydin ME, Kopuz C, Demir MT, Corumlu U, Kaya AH: Localization of pterion in neonatal cadavers: a morphometric study. Surg Radiol Anat. 2010, 32:545-50. 10.1007/s00276-009-0615-7